AN EXPERIMENTAL STUDY OF SULFIDE SCALE FORMATION IN PIPES

Nikolaos Andritsos and Anastasios J. Karabelas

Chemical Process Engineering Research Institute and Department of Chemical Engineering, Aristotle University of Thessaloniki. P.O Box 1517, GR 540 06 Thessaloniki, Greece

Key words: experimental, sulfide scaling, lead sulfide, iron sulfide, cadmium sulfide

ABSTRACT

Results are summarized of an on-going experimental investigation of scale formation in a pipe with four sulfide systems; i.e. PbS, CdS, mixed PbS and CdS, and iron sulfide. The influence of the main system variables (flow velocity. pH, species concentration, temperature) has been established and valuable insight has been gained into the prevailing mechanisms. The data from all four systems are surprisingly similar. They show that appreciable mass of relatively strongly adhering deposits develops only within a narrow pH range, which is associated with the solubility of each sulfide. With increasing pH (and supersaturation), precipitation in the bulk solution occurs immediately after mixing of the metal-rich and sulfide-rich reagent streams, which tends to consume a significant part of metal cations, thus causing a drastic reduction of the driving force for surface crystallization and consequently of the deposition rate. All evidence indicates that the process of scale formation, at least within the narrow pH limits where a significant amount of hard scale develops, is controlled by the convective diffusion of lattice ions to the pipe surface. The implications of the above results, for the development of an appropriate scale control strategy in geothermal systems, is briefly discussed.

1. INTRODUCTION

Several heavy metal sulfides (PbS, ZnS, FeS etc.) are found in scale deposits formed by the flow of high-enthalpy and high-salinity geothermal brines, such as those in Salton Sea, California (Skinner *et al.*, 1967; Austin *et al.*, 1977 and Gallup *et al.*, 1990), in Milos Island, Greece (Andritsos & Karabelas, 1991a), and in Asal, Djibouti (Criaud & Fouillac, 1989). These scales are usually intermixed with amorphous silica or with metal (mostly iron) silicates. Iron sulfide scales are also encountered in several low temperature geothermal systems in the Dogger region (Criaud & Fouillac, 1989). Regarding the iron sulfide scales several crystalline phases have been identified Typical examples include monosulfides such as troilite (Gallup *et al.*, 1990), pyrrhotite (Andritsos & Karabelas, 1991a), mackinawite (Criaud & Fouillac, 1989) and pyrite. All sulfide-rich scales encountered in geothermal plants consist of at least two major sulfides or, in the case of iron sulfide scales, of various polymorphic phases, while the scale composition may vary from location to location. For example, in the Milos geothermal plant and in the geothermal loop experimental facility at Niland, California (Austin *et al.*, 1977), PbS is the main sulfide deposited just downstream of the control valve, while much less galena is found in the scales farther downstream.

The formation of hard and tenacious scales in both the surface and the subsurface equipment of a geothermal installation has inevitably severe adverse consequences on the operation and the economics of the plant. It appears that two methods are applied towards mitigating the scaling problem at high enthalpy/high salinity geothermal installations; the reduction of the brine pH, and the flash crystallization-clarification process. It is reported that both methods provide very good scale control.

The first method, implemented by injection of an acid, has also been proven to offer an effective way to control metal-silicate scaling. Gallup (1989) reports that inhibition of the iron-silicate scales is achieved by reducing the brine pH by only 0.1 to 0.3 units. The injection of an acid into the brine can significantly increase the solubility of sulfides, thus reducing their tendency to precipitate on the pipe walls (Jackson and Hill, 1976; Gallup *et ul.,* 1990).

It is reported (Owen and Michels, 1984; Di Pippo, 1988) that in 1982 at Salton Sea a 10 MW flash unit started successful operation using a crystallization-clarification process. This process for handling and treatment of the brines consists of a system of two flash-crystallizer separators and a reactor-clarifier (which receives the particles generated in the separators), followed by a media filter system.

The scope of the research effort in this laboratory is two-fold: (1) to understand the mechanism(s) of sulfide scale formation by carrying out laboratory experiments in a pipe under controlled conditions, which partly simulate the conditions occurring after flashing, where the brine becomes suddenly supersaturated with respect to several phases, and (2) to develop expertise on methods of mitigating scaling due to sulfides.

The first sulfide system investigated in this laboratory was PbS and most of the results of this investigation are reported in two publications (Andritsos and Karabelas, 1991b and c). It is found that appreciable deposits form within a narrow pH range, closely associated with the solubility of PbS, and, thus, depend upon a number of parameters, such as temperature, lattice ion concentrations and ionic strength (salinity). In this pH range, an increase of liquid velocity and temperature greatly increases the deposition rate. indicating a mass transfer-controlled mechanism. At higher pH values precipitation in the bulk occurs immediately after the mixing of the lead and sulfide solution streams, which tends to consume most of the mailable metal cations, thus causing a drastic reduction of the deposition rate. The PbS particles formed with a zero-salinity liquid have a well-defined prismatic shape, while those obtained with saline liquids exhibited an octahedron shape.

In geothermal plants, as already reported, several sulfide phases coprecipitate at the pipe wall to form the sulfide-rich scales. Consequently, the study of scaling phenomena due to simultaneous precipitation of several metal sulfides may be also of great interest. An experimental study of deposition of mixed sulfides (eg. PbS, FeS, ZnS), however, is hindered by the large differences in solubility (several orders of magnitude) of the various compounds at temperatures close to ambient, and by the fact that at these conditions, amorphous ZnS and FeS (Ricard, 1989) phases may be formed. It is noted that in the Milos case the solubilities of the major scale-forming sulfides at high temperatures (~220°C) differ only by less than an order of magnitude (Helgeson, 1969). At atmospheric conditions, however, the solubility product of these sulfides may vary by several orders of magnitude, as seen in Table 1. Accordingly, the system PbS/CdS was selected for the investigation of *a mixed* sulfide system, since their solubilities are very close at atmospheric conditions. Results of studies on bulk coprecipitation of several binary sulfide systems have recently appeared in the literature (Wilhelmy and Matijević, 1985; Abrahams and Huiocchi, 1988). The CdS system was also investigated independently (Andritsos and Karabelas, 1994). CdS is

rarely encountered in geothermal scales. However, it is perhaps the best investigated sulfide, because of its important role in photocatalytic energy conversion.

Table 1. Solubility products (pK_{sp}) of various scale-forming sulfides and the second dissociation constant, pK_2, of H_2S at atmospheric conditions

Sulfide	Helgeson (1969),	Hamilton *et al.*	Smith and Martell	Licht (1988),
PbS				32.5
FeS	18.9	188	181	21.0
ZnS(1)	25.7		24.7	28.9
ZnS(2)	23.7		22.5	26.1
$CuFeS_2$	61.5			-
CdS		28.5	27.0	33.3
H_2S	13.9	13.9	13.9	17.3

(1) Sphalerite, (2) Wurtzite

The study of iron sulfide scale formation is also of great importance since it is the most abundant component in sulfide-rich scales. Despite the fact that the iron-sulphur system is perhaps the most extensively studied binary sulfide system, the laboratory synthesis and the identification of the various phases have encountered considerable difficulties. Pyrite is the most stable phase, but several other phases may occur, some of them metastable, at low temperatures. Taylor (1980) reports that above 200°C only a few sulfide phases are stable (pyrrhotite and pyrite), while at atmospheric conditions several phases are expected to occur. The reaction between sulfide species and ferrous ions at atmospheric conditions and close to neutral pH leads to the precipitation of a black iron (II) sulfide (Morse *et al.*, 1988; Ricard, 1989), that slowly transforms to mackinawite. This initial product is seemingly an amorphous precipitate prone to oxidation.

Various parameters are expected to affect the scaling process. Flow velocity, supersaturation ratio (or pH), species concentration, temperature, and material of the substrate are parameters investigated in this laboratory. In this paper the results of all sulfide systems investigated so far are presented in a unified way, while new data are reported on mixed sulfides (PbS and CdS) and on the iron sulfide system.

2. EXPERIMENTAL

A detailed description of the experimental set-up and procedure for carrying out the sulfide deposition experiments in tubes is given in Andritsos and Karabelas (1991b). Some minor modifications were made for the runs with CdS, mixed sulfides and iron sulfide. A schematic diagram of the set-up is shown in Figure 1. Tap water is used in all experiments, since large quantities of water are required for the once-through experiments. However, our studies show that no species (other than the reacting ones) has any contribution to the scale formed for pH less than 8. Water is drawn either directly from the mains or from a 1.5-m^3 tank, used for the preparation of saline solutions. The water flow is measured by a SIGNET 2530 flow sensor, while a flow controller system maintains a constant flow. After passing through an electric heater, the water at a fixed flow rate and temperature is split in two streams. Two FMI dosimetric pumps regulate the flow of concentrated reagent solutions into the two streams. The pH of the final solution is controlled by injecting reagent grade nitric acid into the metal stream and by employing a MARK IV 2031 pH controller system. The pH is also monitored externally by a Metrohm Model 632 pH-meter. The test section is located 1.2 m downstream from the point of mixing of the two streams. The test section consists of four to six tubular units, each holding two replaceable pairs of semiannular coupons, forming a pipe section with a uniform inner diameter of 13 mm. In the PbS and CdS runs a second test section was used, located 10 m downstream from the first test section.

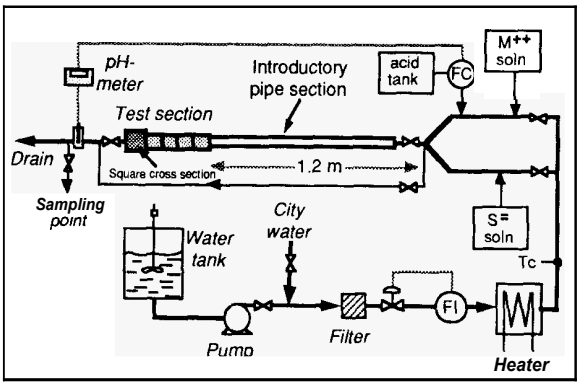

Figure 1. Schematic diagram of the experimental setup.

Another special test section, which is used to hold small rectangular coupons suitable for scanning electron microscopy (SEM) examination, follows the main test section. It consists of two 6-cm long tubular segments. The coupons are made of 316L stainless steel and of teflon. The former coupons were diamond polished to obtained a smooth, mirror-like surface.

Reagent grade lead nitrate, cadmium nitrate, ferrous ammonium sulphate and sodium sulfide (Merck) were used for the preparation of the respective reagent solutions. The metal solutions were frequently standardized by atomic absorption spectroscopy, while the sulfide solutions were checked by titration with mercuric acetate using dithizone indicator. Freshly prepared metal and sulfide solutions were always used.

The crystal structure of the deposits was established by X-ray diffraction using the K_α line of Cu in a Siemens Model D500 diffractometer. The morphology of the deposits (on coupons) was examined by SEM in a JEOL, JSM-840A unit. The shape and size of bulk precipitated sulfide particles was also examined by SEM on 0.2 μm polycarbonate membranes (Millipore®). The coupons and the membranes were carbon coated prior to observation. Qualitative chemical analysis of the deposits was performed by energy dispersive spectrometry in a LINK AN10000 system.

Light absorbance measurements in a HITACHI U-3200 spectrophotometer were used for monitoring bulk precipitation of the flowing solution. The zeta-potential of PbS and CdS deposit particles and of bulk precipitated particles was determined in a microelectrophoretic apparatus (Rank Brothers, model MKII). The morphology and size of bulk precipitated particles was examined by SEM on 0.2 μm polycarbonate membranes. For the FeS system dynamic light scattering measurements of particle size were carried out in a Brookhaven Instruments Co. system.

3. DEPOSITION RESULTS

3.1 Temporal Evolution of Deposits

The range of the various parameters examined is presented in Table 2 for each sulfide system investigated. The effect of salinity (or of ionic strength), by adding NaCl, was investigated only with the PbS system in the range of 0 to 2 M NaCl. The initial total sulfide concentration was in approximately stoichiometric ratio with that of the metals.

Table 2. Range of experimental conditions

Variable	PbS	CdS		
pH	1-4	1-4		
Flow velocity, m/s	0.2-1.0	0.2-2.0		*0.5,* 1.0
Metal conc., mM	0.005-0.11	-	Pb: 0.05	0.15-0.25
		-	Cd: 0.11	
Temperature, °C	20-50	20-50		15-50
Salinity, M *NaCl*	0-2	-		
Substrate	304-316L SS, teflon	316L SS, teflon	316L SS, teflon	316L SS. teflon

Figure 2 presents typical deposit (scale) mass vs. time curves for several cases on stainless steel coupons. It is a common feature of all systems examined that for each run a linear relationship exists between the mass of deposits and time. The slope of this straight deposition (scale formation) line defines the initial deposition rate. No induction (or delay) period is observed for all cases, in contrast with some reported data on deposition of other sparingly soluble salts (Hasson, 1981). It is characteristic of all systems and conditions that the mass of deposits collected on teflon coupons is almost always slightly higher than that on stainless steel by 0-15%.

Microscopically, the deposit formation process for all systems proceeds as follows: At very short times after a run starts (1-2 min), isolated and very small particles, usually less than 200 nm, are observed on the substrate. At all stages the simultaneous wall crystallization and deposition of bulk precipitated particles cannot be excluded. However, the almost zero values of light absorbance of samples from the flowing liquid suggest that bulk precipitation and subsequent deposition is insignificant. The number of particles per unit area ana the size of the initially observed particles, compared for the same elapsed time, are affected by the pH (or the level of superasaturation) for the CdS and PbS systems. The lower the pH the smaller the number of particles per unit area and the larger their size. Further deposit formation occurs due to growth of isolated particles, which (with the exception of PbS deposits from zero-salinity liquids) led to the formation of a coherent layer covering the entire pipe surface. A similar description of deposit formation due to other scaling compounds is given by Sohnel and Garside (1992).

3.2. pH Dependence

Appreciable deposition for a certain set of experimental conditions (constant species concentration, temperature, salinity and velocity) is confined to a narrow range of pH values, as shown in Figure 3 for three cases. A smking feature of the deposition curve is its "bell" shape. Starting from low pH values the deposition rate increases significantly up to a maximum rate. In the pH range of the increasing part of the deposition curve the flowing liquid inside the test section is still clear (and the light absorbance measurements of samples give zero readings), indicating that no precipitation occurs in the bulk. Under these conditions the deposit formation takes place via sulfide crystallization right onto the pipe wall. As the supersaturation level increases (with the pH) bulk precipitation is observed almost instantly after mixing the two reagent streams. Bulk precipitation consumes a large portion of the metal and sulfide ions, thus reducing the driving force for crystallization on the tube wall. Sulfide particles and aggregates formed in the bulk can be deposited onto the tube surface (or on the coherent deposit layer), but at very small rates and do not contribute to the deposit layer. These deposits, called loose deposits, adhere very weakly on the pipe surface and can be readily detached by fluctuating fluid flow stresses. At even higher supersaturation levels only a scanty mass of loose deposits are observed on the substrate.

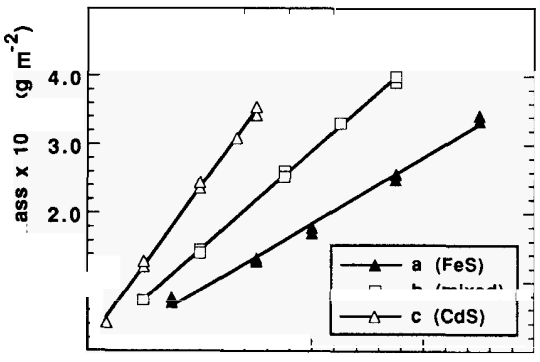

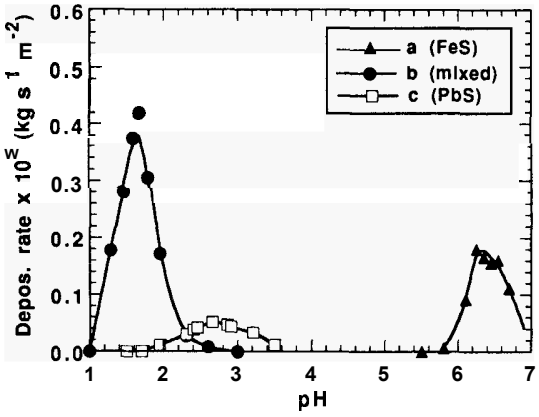

Figure 3. Effect of pH on the deposition rate. (a) $[Fe]_t$=0.25 mM, T=30°C, U=0.5 m s^{-1}; (b) $[Pb]_t$=0.06 mM, $[Cd]_t$=0.11 mM, T=25°C, U=0.46 m s^{-1}, and (c) $[Pb]_t$=0.015 mM, T=25°C, U=0.46 m s^{-1}.

3.3. Flow Velocity Effect

The deposition rate of all sulfides for a fixed pH value and species concentration is greatly affected by the flow velocity. The deposition rate depends on flow velocity to a power of 0.8 to 0.9 (Andritsos and Karabelas, 1991b and 1994). However, it appears that the velocity has no effect on the deposit morphology.

3.4. Temperature Effect

An increase of the temperature of the liquid tends to significantly increase the deposit formation rate, as illustrated in Fig. 4, possibly through an increase of the transport rate of the scale building ions to the pipe wall. The temperature data correspond approximately to the maximum deposition rate. The pH of the maximum rate shifts to higher pH values with temperature for the PbS and CdS systems (the solubility of both sulfides increases with temperature), while the pH of the maximum rate for the FeS system remains virtually unaffected by temperature.

3.5. Morphology and Characterization of Deposits

Morphologically, the sulfide systems of this investigation can be categorized in two groups; i.e. those with a rather coherent deposit layer, and those exhibiting growth of discrete particles fixed on the wall. Only PbS deposited from zero-salinity liquids belongs to the second group.

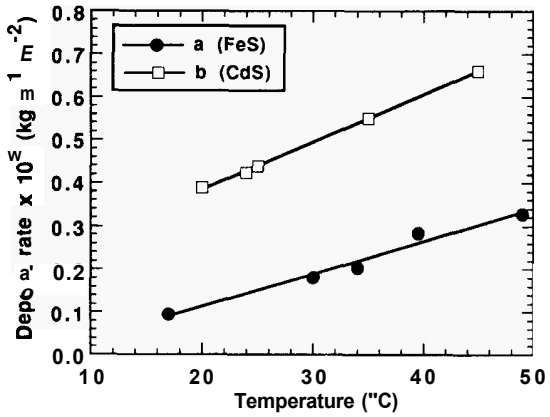

Figure 4. Effect of the liquid temperature on the deposition rate, (a) $[Cd]_t$=0.16 mM, U=0.46 m s^{-1}; (b) $[Fe]_t$=0.25 mM, U=0.5 m s^{-1}.

Figure 5 shows micrographs of PbS deposits from a zero-salinity and a 0.5 M NaCl liquid. In the top picture the PbS particles have a well-defined prismatic shape which is preserved throughout the deposit formation process. On the other hand, the presence of chloride ions in the solution (bottom picture) promotes the formation of octahedron-shaped crystals. With deposit growth, the initially isolated particles come in contact and each particle seems to fuse with neighboring ones. This kind of contact among the particles results in the formation of a compact layer which adheres quite strongly on the substrate. The color of all PbS deposits is gray and the X-ray diffraction analysis of the deposits gives the pattern characteristic of galena.

The CdS deposits resemble those of PbS obtained from saline waters, forming a rather coherent and compact layer over relatively short times. **A** micrograph of a CdS deposit layer is illustrated in the top picture of Figure *6.* The first CdS particles have a nearly spherical shape with a rough surface. The color of these deposits varies from dark orange to yellow, depending on pH. The XRD pattern of the deposits exhibits the characteristic lines of greenockite (α-CdS). Surface analysis by EDS does not show the presence of any element other than Cd and **S.**

The mixed PbS-CdS deposits (middle picture, Fig. 6) consist of discrete cubic PbS crystals (with some degree of interpenetration) and of rough sphere-like CdS particles which at later stages form a coherent layer. Although chemical analysis of mixed deposits showed that the Cd to Pb ratio is close to 1 (on a weight basis), the X-ray data show only well-defined peaks belonging to galena.

For the FeS system it is observed that a black amorphous phase is formed for pH values greater than about 6. It is not possible to clearly define the nature of these deposits. However, a phase with similar characteristics precipitating in the above pH range is identified as amorphous iron (II) sulfide in the literature (Berner, 1964; Ricard, 1989), which can be considered as a precursor phase for mackinawite. The deposits are prone to oxidation, as indicated by the change of black color to reddish-brown after air exposure. XRD examination of both black and reddish-brown deposits do not reveal any crystalline phase, other than some small peaks belonging to sulfur *(a-S).* Analysis of the deposits by EDS shows qualitatively that the major constituents of the deposits are iron and sulfur. The presence of calcium can also be detected, probably adsorbed on the deposits or from the evaporation of water droplets on the coupons. **A** micrograph of FeS deposits is shown in Fig. 6 (bottom picture), **A** distinct feature of the FeS deposit layers is the existence of sphere-like protrusions. Some of these protrusions seem to have been ruptured in a manner reminiscent of bursting due to trapped gas.

4. CHARACTERIZATION **OF BULK** PRECIPITATED PARTICLES

The objective of this part of the work is to characterize the sulfide particles which are precipitated in the bulk in order to better understand the decline of wall crystallization rate at relatively high supersaturation levels and to assess the crystallization-clarification process for mitigating the sulfide scaling problem.

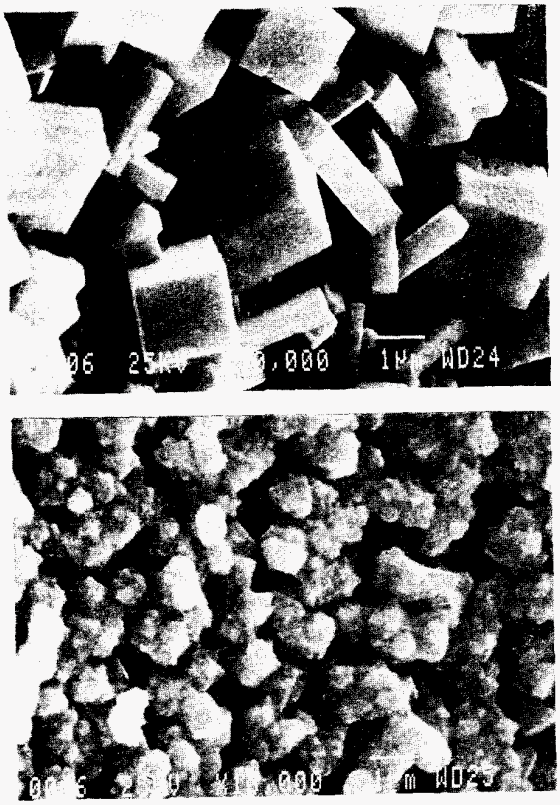

Figure 5. Morphology of PbS deposits for U=0.46 m s^{-1}. Upper: $[Pb]_t$=0.07 mM, T=25°C, pH=1.7, time=1.8 h, *zero* salinity. Lower: $[Pb]_t$=0.11 mM, T=25°C, pH=1.8, time=4 h, in a 0.5 M NaCl medium.

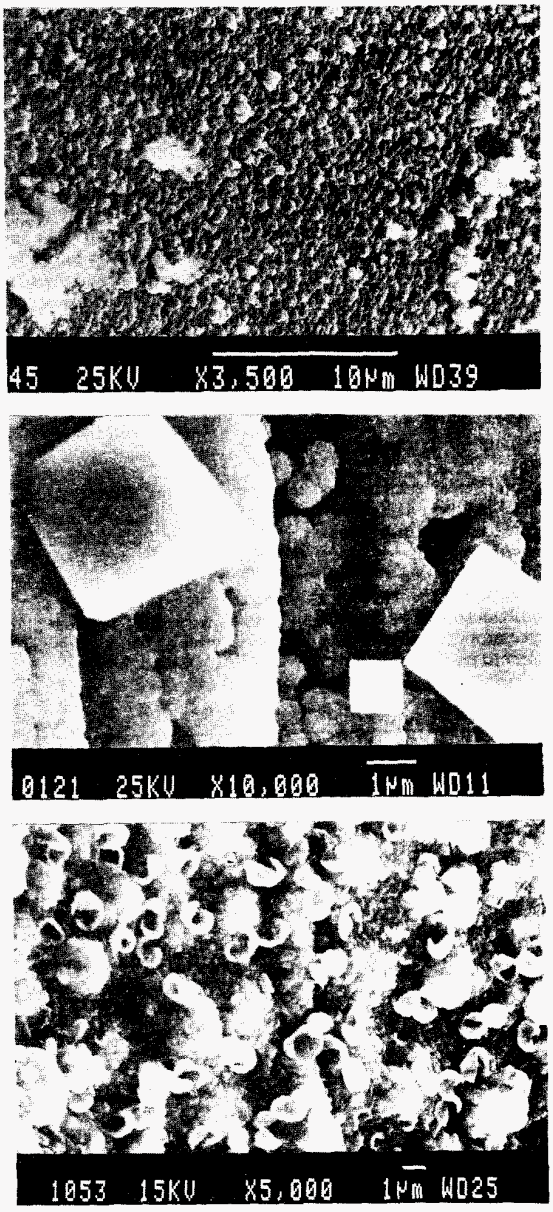

Figure 6. Morphology of sulfide deposits. Upper: CdS, $[Cd]_t$=0.16 mM, T=25°C, time=2 h, U=0.46 m s^{-1}; **Middle:** mixed. $[Pb]_t$=0.06 mM, $[Cd]_t$=0.11 mM, T=25°C, time=2.6 h, U=0.46 m s^{-1}; Lower: amorphous FeS, $[Fe]_t$=0.25 mM, T=30°C, time=3.5 h, U=0.5 m s^{-1}.

The shape of bulk precipitated sulfide particles, for all systems studied, is in general similar to those observed in the deposits. The PbS particles precipitating from zero-salinity liquids exhibit a cubic shape and those from saline liquids an octahedral shape, with a broad size distribution. The largest PbS particles obtained at relatively low supesaturation levels after aging for several hours are about 5 μm, while at high supersaturation levels the particles are smaller than **0.1** μm. The measured zeta-potential of bulk precipitated particles is close to zero for the pH range of 1 to **4.**

The bulk precipitating CdS particles are spherical in shape and of relatively narrow size distribution. In general, the surface of the larger particles is not very smooth. The size of the spherical particles depends on pH, or more precisely on the supersaturation ratio. At low supersaturation levels, the particle diameter is of the order of 1 μm, while at higher levels (in the region of practically zero deposition rates) the size is less than 0.1 μm. Zeta-potential measurements at 25°C, performed on particles precipitated in the bulk and on particles recovered from the deposit layer, give an i.e.p. around 3. The zeta-potentials seem to be independent of the particle formation process (wall crystallization or bulk precipitation) and of the mean particle diameter.

The initial mean diameter of FeS bulk precipitated particles in the pH range of 6-7 (measured by DLS) is about 100 nm. Measurements of the particle size cannot be carried out in a time shorter than 2 min after the sol preparation. Generally, the particle size tends to increase, rather slowly, with time. SEM examination of particles collected on polycarbonate filter membranes reveals that the particles are roughly spherical in the range of 50-200 nm. The increase of the mean size with time may be attributed to coagulation rather than to individual particle growth.

5. DISCUSSION

The thermodynamic driving force for scale formation (and for bulk precipitation) is the change of the Gibbs free energy

$$AG = - RT \ln S \quad (1)$$

where R is the gas constant, T is the absolute temperature and S is the saturation ratio, which for the metal sulfides of the present study is defined as

$$S = \left[\frac{(M^{2+})(S^{2-})}{K_{sp}}\right]^{1/2} \quad (2)$$

Quantities in parentheses denote the activities of the respective species, M corresponds to Pb, Cd or Fe and K_{sp} is the thermodynamic solubility product of the sulfide solid phase.

Since pH is directly related to S, a plot of deposition rate vs. *S* should offer a direct comparison of all sulfide systems. Such a plot is presented in Fig. 7, for the three sulfides studied and for approximately the same mass concentration, considering that all total metal concentration is converted to the corresponding sulfide. The **S** value for the FeS system refers to mackinawite. The ratios are computed by using the HYDRAQL code (Papelis *et al.*, 1988). All but the following thermodynamic stability constants are from Smith and Martell (1976). For CdS: pK_{sp}=28.5 (Hamilton ***et al.***, 1969) and for mackinawite: pK_{sp}=17.5 (Berner, 1967).

In this figure, an interesting qualitative feature is evident; i.e., for scale formation to occur, a critical value of the supersaturation ratio, S_c, should be exceeded. This critical value appears to be lower than the value corresponding to spontaneous precipitation, at least for the short fluid residence times of the present experiments. With increasing supersaturation above S_c, the measured deposition rate rises significantly reaching a maximum value. At even greater S values, spontaneous bulk precipitation occurs instantly with mixing of the two reagent streams. In fact, Ricard (1989) reports that for the FeS system in the pH range of 7 to 9, bulk precipitation is almost complete in 0.26 **s** after mixing the reagent streams. Consequently, the supersaturated sulfide solutions are quickly depleted of most of the scale forming ions, which otherwise could be transported to the pipe walls and take part in scale formation. The sulfide particles formed in the bulk (with size of order of 100 nm) could be deposited on the pipe surface, but simple calculations with accepted correlations show that the convective transport rate of the particles is two orders of magnitude smaller than that of individual ions.

Another point of interest is the lower value of the maximum rate for the FeS system compared with those of PbS and CdS (Fig. 7). This may be adequately explained by the mechanism considered by Ricard (1989) that in the FeS system the initial precipitate is a gel approaching the composition $Fe(SH)_2$, which quickly loses sulfide species and amorphous FeS begins to appear.

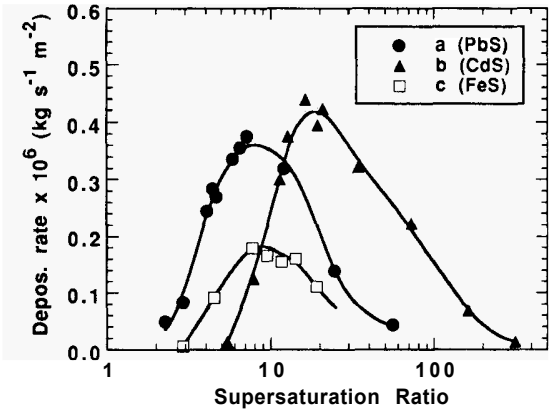

Figure 7. Effect of the supersaturation ratio on the deposition rate. (a) $[Pb]_t$=0.11 **mM**, T=25°C, U=0.46 **m** s^{-1}; (b) $[Cd]_t$=0.16 mM, T=25°C, U=0.46 **m** s^{-1}, and (c) $[Fe]_t$=0.25 **mM**, T=30°C, U=0.5 **m** s^{-1}.

For the wall crystallization process the controlling step may be either the mass transfer of lattice ions to the tube surface or a number of elementary processes grouped under the term "surface reaction" process. Hasson (1981) concludes that the formation of $CaCO_3$ deposits in pipes is largely a diffusion-controlled process, while Sohnel and Garside (1992) in reviewing scale formation report that it is usually controlled by a surface reaction mechanism. Considering the former mechanism, the expression for the net flux of metal ions, M^{++}, to the pipe wall (or to already formed crystals on the substrate) is given as

$$J_M = k_D ([M^{++}]_o - [M^{++}]_{eq}) \quad (3)$$

where $[M^{++}]_o$ is the bulk and $[M^{++}]_{eq}$ the equilibrium metal ion concentration and k_D a convective mass transfer coefficient. One can use a plethora of available expressions to compute the transfer coefficient, For example, Papavergos and Hedley (1984) suggest

$$k_D = 0.07\, u^* Sc^{-2/3} \quad (4)$$

where Sc is the Schmidt number (ν/D), ν the kinematic viscosity, D the diffusion coefficient of the ions, u^* the friction velocity ($u^* = U\sqrt{f/2}$) and f the friction factor. Thus k_D can be adequately predicted, provided that the diffusion coefficient of metal ions is known. The flux of metal ions should be equal to the flux of all sulfide species present in the solution

$$J_M = J_{S,t} = J_{S^{2-}} + J_{HS^-} + J_{H_2S} \quad (5)$$

Because of the complexity of eq. (5) and the uncertainties in the estimation of the mass transfer coefficients for the sulfide species, predictions of deposition rates can be made based on the metal ion transport only. The literature suggests that ionic diffusion coefficients for divalent cations are about 1×10^{-5} cm^2/s (Cussler, 1984).

A transport controlled mechanism appears to adequately explain the effects of flow velocity and temperature on the deposition rate. The dependence of this rate upon the flow velocity can be written as $U^{0.875}$, as indicated in eq. **(4)** .This exponent is close to those found experimentally. Furthermore, the estimated activation energies for the three sulfide systems, calculated from the temperature data, give values close to 20 kJ mol-1. This value is indicative of a diffusion controlled mechanism (Nancollas, 1983). It is noted that the temperature data correspond to superasaturation ratios far away from the critical ones.

At this point, referring to Fig. 7 and to eq. (3), one may pose two questions; first, how the existence of the critical supersaturation ratio can be taken into account in modeling and, second, how one may obtain information on the critical value S_c of a certain precipitating system, without resorting to difficult laboratory runs. There is no obvious answer to the second question. The answer to the first question is that probably at low supersaturation ratios a surface-controlled mechanism is operative, which has to be taken into account in combination with the convective diffusion mechanism. It is well known that the crystallization rate due to a surface mechanism is orders of magnitude smaller than that due to a diffusion mechanism (Nielsen and Toft, 1984). Thus, even if at

low supersaturation ratios there is deposit formation only due to a surface mechanism, the small mass of deposits would be impossible to weigh.

6. CONCLUDING REMARKS

The data from all four sulfide systems show that deposits form essentially only within a narrow pH range, which is associated with the solubility of each sulfide. At relatively large supersaturation ratios precipitation in the bulk solution occurs immediately after mixing of the two reagent streams, thus depleting the solution of metal ions needed for wall crystallization. All evidence points to a convective diffusion-controlled process, at least within the narrow pH range where a significant amount of hard scale develops.

By taking into account the experimental results and the previous discussion the following comments can be made regarding the two principal methods for mitigating the sulfide scaling problem, assuming that the high temperature and pressure of the real brines do not significantly alter the present findings. (a) A small reduction of pH of the produced brine can be beneficial, not only by converting a supersaturated solution to an undersaturated one, but also by decreasing the supersaturation ratio below its critical value. (b) A small increase **of** pH can alter the spontaneous precipitation propensity of a brine, while the relatively small size of the precipitated particles may suggest the use of a flocculating agent in the clarification system

ACKNOWLEDGMENTS. Grateful acknowledgment is made **of** financial support **from** the Commission **of** European Communities under contracts No JOUG-0005-C and No JOU2-CT92-0108. The authors wish to thank Prof. S. Sklavounos, Dr. **E.** Pavlidou and Mr. V. Kyriakopoulos for the **SEM** pictures.

REFERENCES

Abrahams, M.S. and Buiocchi, C.J. (1988). Nucleation of precipitates of ZnS and (Zn,Cd)S for phosphor synthesis. ***J. Electrochem. Soc.***, Vol. 135, pp 1578-1583.

Andritsos, N. and Karabelas, A.J. (1991a). Sulfide scale formation and control: the case of lead sulfide. ***Geothermics,*** Vol. 20, pp. 343-353.

Andritsos, N. and Karabelas, A.J. (1991b). Crystallization and deposit formation of lead sulfide from aqueous solutions I. Deposition rates. ***J. Colloid/Interface Sci.***, Vol. 145, pp. 158-169.

Andritsos, N. and Karabelas, A.J. (1991c). Crystallization and deposit formation of lead sulfide from aqueous solutions II. Morphology of deposits. ***J. Colloid Interface Sci.,*** Vol. 145, pp. 170-181.

Andritsos, N. and Karabelas, A.J. (1994). Growth of CdS films from aqueous solutions. ***J. Colloid Interface Sci.,*** **Vol.** 165, pp. 301-309.

Austin, A.L., Lunberg, A.W., Owen, L.B. and Tardiff, G.E. (1977). ***The LLL Geothermal Status Report, January 1976 - January 1977.*** Report UCRL-50046-76, Lawrence Livermore Laboratory, Livermore, CA. 173pp.

Criaud, A. and Fouillac, C. (1989). Sulfide scaling in low enthalpy geothermal environments: A Survey. ***Geothermics,*** Vol. 18, pp 73-81.

Cussler, E.L. (1984). ***Diffusion - Mass Transfer in Fluid Systems.*** Cambridge University Press, New York, 525pp.

Di Pippo, R. (1988). International developments in geothermal power production. ***Geothermal Resources Council Bulletin,*** May, pp. 8-20.

Gallup, D.L. (1989). Iron silicate scale formation and inhibition at the Salton Sea geothermal field. ***Geothermics,*** Vol. 18, pp. 97-104.

Gallup, D.L., Andersen, G.R. and Holligan, D. (1990). Heavy metal scaling in production well at the Salton Sea geothermal field. ***Geothermal Resources Council Transactions,*** Vol. 14, pp. 1583-1590.

Hamilton, L.F., Simpson, **S.G.** and Ellis, D.W. (1969). ***Calculations*** of ***Analytical Chemistry.*** Mc-Graw Hill, New York, 7th ed. 511pp.

Hasson, D. (1981). Precipitation Fouling. In: ***Fouling*** of ***Hear Transfer Equipment,*** E.F.C. Somerscales and J.G. Kundsen (Eds), Hemisphere Publ. Co., Washington, pp. 527-568.

Helgeson, H.G. (1969). Thermodynamics of hydrothermal systems at elevated temperatures and pressures. ***Am. Jour. Sci.***, Vol. 267, pp. 729-804.

Jackson, D.D. and Hill, J.H. (1976). ***Possibilities for controlling heavy metal sulfides in scale from geothermal brines.*** Report UCPL-51977, Laurence Livermore Lab., Livermore, CA. 14pp.

Morse, J.W., Millero, F.J., Cornwell, J.C. and Rickard, D. (1987). The chemistry of hydrogen sulfide and iron sulfide systems in natural waters. ***Earth-Science Reviews,*** Vol. 24, pp. 1-42.

Nancollas, G. (1983). Nucleation and growth of scale crystals. In: ***Fouling of heat exchanger surfaces,*** R.W. Bryers (Ed.), Engng Foundation, New York, pp. 531-544.

Nielsen, A.E., and Toft, J.M. (1984). Electrolyte crystal growth kinetics. ***J. Crystal Growth,*** **Vol.** 67, pp. 278-288.

Papelis, C., Hayes., K.F., and Leckie, J.O. (1988). ***HYDRAQL.*** Technical Report No **306,** Stanford University, Stanford, CA.

Rickard, D. (1989). Experimental concentration-time curves for the iron (II) sulfide precipitation process in aqueous solutions and their interpretation. ***Chem. Geol.,*** Vol. 78, pp. 315-324.

Skinner, B.J., White, D.E., Rose, H.J. and Mays, R.E. (1967). Sulfide associated with the Salton Sea Geothermal brine. ***Econ. Geol.,*** Vol. 62, pp 316-330.

Sohnel, **O.** and Garside, J. (1992). ***Precipitation. Basic Principles and Industrial Applications.*** Butterworth-Heinemann, Oxford. 391pp.

Taylor, P. (1987). The stereochemistry of iron sulfides - a structural rationale for the crystallization of some metastable phases from aqueous solutions. ***Am. Miner.,*** Vol. 65, pp. 1026-1030.

Wilhelmy, D.M. and Matijević, E. (1985). Preparation of uniform colloidal particles of lead sulfide and of mixed sulfides of cadmium+zinc and cadmium+lead. ***Colloids and Surfaces,*** Vol. 16, pp. 1-8.